Kinematic analysis of a single-loop reconfigurable 7R mechanism with multiple operation modes

Xiuyun He, Xianwen Kong, Damien Chablat, Stéphane Caro, Guangbo Hao

Kinematic analysis of a single-loop reconfigurable RRRR-RRR mechanism with multiple operation modes

Xiuyun He†, Xianwen Kong†,*, Damien Chablat‡, Stéphane Caro‡, Guangbo Hao§

†*School of Engineering and Physical Sciences, Heriot-Watt University, Edinburgh, EH14 4AS, UK*

‡*Institut de Recherche en Communications et en Cybernétique de Nantes (IRCCyN), Université Nantes Angers Le Mans, Nantes, France*

§*Department of Electrical and Electronic Engineering, School of Engineering, University College Cork, Cork, Ireland*

ABSTRACT

This paper deals with the kinematic analysis of a single-loop reconfigurable RRRR-RRR mechanism with multiple operation modes (SLR7RMMOM), which is composed of seven revolute (R) joints and can switch from one operation mode to another one without disconnection and reassembly. The algorithm for the inverse kinematics of the serial open 6R chain using kinematic mapping is adopt to deal with the forward kinematics for the SLR7RMMOM. 13 sets of solutions for the SLR7RMMOM are computed. Among these solutions, nine sets are real solutions, which are verified using the CAD models of the mechanism. It is shown that the present mechanism has three operation modes: translational mode and two 1-DOF planar modes. The transitional configurations between the three modes are also identified.

KEYWORDS: *Single-loop reconfigurable mechanism; Multiple operation modes; Forward kinematics; Kinematic mapping; Transitional configuration*

1. Introduction

Reconfigurable parallel mechanisms (RPMs) have been received increasing attention from researchers around the world. One class of RPMs can generate different operation modes to fulfil variable tasks based on a sole mechanism. Different approaches have been proposed to design RPMs generating multiple motion patterns. Several classes of RPMs have been developed such as modular reconfigurable mechanisms,[1,2] metamorphic mechanisms,[3] kinematotropic mechanisms,[4] variable actuated mechanism,[5] and reconfigurable mechanisms with multiple operation modes. This paper focuses on a reconfigurable mechanism with multiple operation modes since this class of RPMs can be reconfigured without disassembly and without increasing the number of actuators. A systematic approach has been proposed[6,7] for the synthesis of reconfigurable mechanisms with multiple operation modes, including single-loop reconfigurable mechanisms with multiple operation modes[6] and multiple-loop reconfigurable mechanisms with multiple operation modes.[8]

Meanwhile, several approaches have been developed to deal with the kinematics and singularity analysis of serial and parallel mechanisms, such as different evaluation algorithm,[9] screw theory algorithm[10] and kinematic mapping algorithm.[12] Husty and Pfurner have made a significant contribution to the algebraic approach to the kinematic analysis of mechanisms.[11-13] It has been shown that algebraic method is very efficient for both direct (forward) and inverse kinematic analysis of mechanisms.

This paper aims to analyze a single-DOF (degree-of-freedom) single-loop reconfigurable RRRR-RRR mechanism with multiple operation modes (SLR7RMMOM) using the effective algorithm for the inverse kinematics of a general serial 6R manipulator. Here R denotes a revolute joint. The operational modes and transitional configurations will be identified. The paper is organised as follows. Section 2 describes the 1-DOF SLR7RMMOM. In Section 3, the forward kinematics analysis for the mechanism is undertaken within three steps mainly using the kinematic mapping method, and the solutions with respect to one given input angle are verified using CAD software. Based upon the results from Section 3, a series of input angles are given and the operation modes and transitional configurations are obtained in Section 4. Finally, conclusions are drawn.

2. Description of a 1-DOF SLR7RMMOM

It is well known that the Sarrus linkage (Fig. 1(a)), which is composed of two groups of three R joints with parallel joint axes (rotational axes), is used to control the 1-DOF translation of the moving platform along a straight line with respect to the base. Since the Sarrus linkage is an overconstrained mechanism, we can insert one additional R joint between the two joints of a link to obtain a non-overconstrained 1-DOF single-loop RRRR-RRR mechanism (Fig. 1(b)).[14] Such a mechanism must have at least two operation modes. In the translational operation mode, it works as the Sarrus linkage in which the moving platform translates along a straight line (Fig. 1(b)). In the 1-DOF planar operation mode, the moving platform undergoes a 1-DOF general planar motion (Fig. 1(c)). Therefore the above RRRR-RRR mechanism is a SLR7RMMOM.

In this SLR7RMMOM, link 7 is the base, and link 4 is specified as the moving platform. Links 4 and 7 are identical and the link lengths and the axes of the R joints must satisfy the following conditions:

$$\mathbf{R}_1//\mathbf{R}_3//\mathbf{R}_4\perp\mathbf{R}_2, \quad (1)$$

$$\mathbf{R}_5//\mathbf{R}_6//\mathbf{R}_7, \quad (2)$$

$$a_1+a_2=a_3=a_5=a_6 \quad (3)$$

where $\mathbf{R}_i$ (i=1,2, …,7) is the unit vector along the axis of joint R_i, and a_i is the link length as indicated in Fig. 1(c).

*Corresponding author. Email: X.Kong@hw.ac.uk.

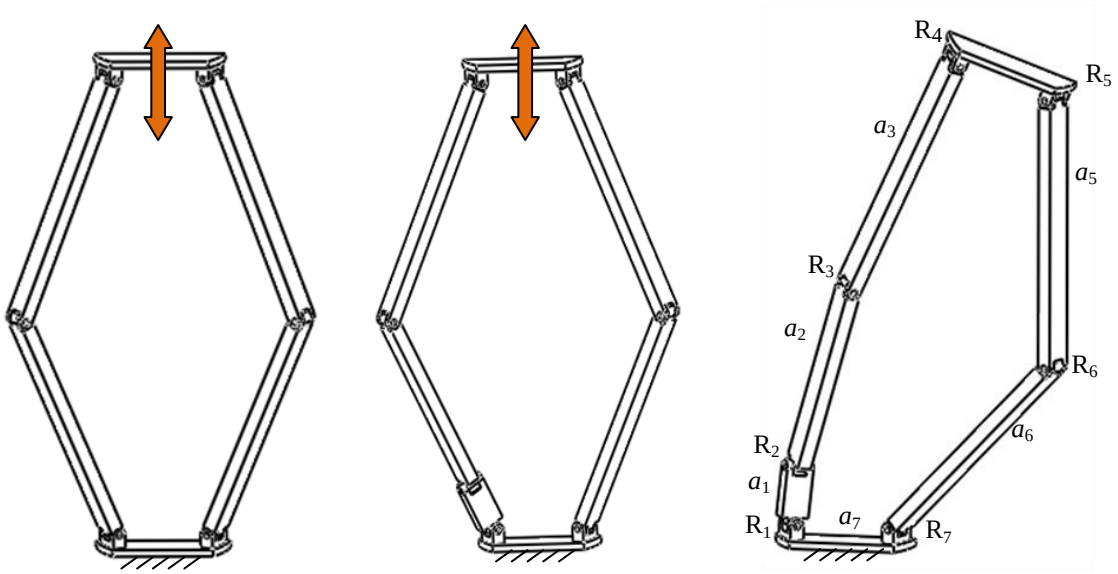

(a) Sarrus linkage (b) SLR7RMMOM in translation mode (equivalent to Sarrus linkage) (c) SLR7RMMOM in 1-DOF planar mode

Fig. 1. Construction of a SLR7RMMOM

The SLR7RMMOM has at least two operation modes. Whether it has additional operational modes is unclear from only the construction of the mechanism. In the next section, we will discuss the kinematic analysis of the SLR7RMMOM in order to identify all of its operation modes as well as transition configurations that the mechanism can switch from one operation mode to another.

3. Kinematics Analysis and Numerical Example

Using the approach to the inverse kinematics for the general 6R mechanism, [11-13] one can perform the kinematic analysis of the SLR7RMMOM. Then all the operation modes and transition configurations of the mechanism can be identified.

3.1. D-H Parameters for the mechanism

In order to define the transformation relations between the links, the coordinate frames Σ_i is attached to link i as follows: the z_i-axis coincides with the axis of joint R_i, the x_i-axis aligns with the common perpendicular to the z_{i-1}- and z_i-axes, and the y_i-axis is defined by the right-hand rule (Fig. 2). With this notation one could write the transformation matrix ($\boldsymbol{T}_i$) from Σ_i to Σ_{i+1} as:

$$\boldsymbol{T}_i = \boldsymbol{M}_i\boldsymbol{G}_i = \begin{bmatrix} 1 & 0 & 0 & 0 \\ 0 & \cos(\theta_i) & -\sin(\theta_i) & 0 \\ 0 & \sin(\theta_i) & \cos(\theta_i) & 0 \\ 0 & 0 & 0 & 1 \end{bmatrix} \begin{bmatrix} 1 & 0 & 0 & 0 \\ a_i & 1 & 0 & 0 \\ 0 & 0 & \cos(\alpha_i) & -\sin(\alpha_i) \\ d_i & 0 & \sin(\alpha_i) & \cos(\alpha_i) \end{bmatrix} \quad (4)$$

where θ_i and d_i are the revolute angle and distance between the two x-axes of links i and i+1, respectively, and α_i and a_i are the twist angle and distance between the two z-axes of links i and i+1, respectively.

The SLR7RMMOM can be regarded as a 6R serial mechanism (Fig. 3(a)) with link 6 as the end-effector (EE), the coordinate frame on which is set as follows. Its z-axis (z_{EE}) coincides with the axis of joint R_7 and its x-axis aligns with the common perpendicular to the z_6-axis and the z_{EE}-axis. The angle between the x_{EE}-axis and the vertical line (θ) is defined as the input angle of the SLR7RMMOM. The D-H parameters of the 6R mechanism are shown in Table 1, which should satisfy the conditions given in Section 2.

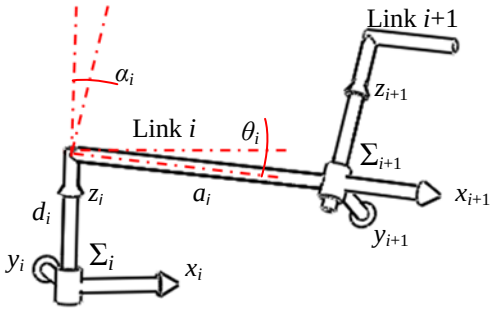

Fig. 2. D-H parameters (Σ is the coordinate frame system)

Table 1. D-H parameters for the loop

i	a_i	d_i	α_i	θ_i
1	0.80	0	90^0	θ_1
2	3.00	0	-90^0	θ_2
3	3.80	0	0^0	θ_3
4	0	1.47	-120^0	θ_4
5	3.80	1.47	0^0	θ_5
6	3.80	0	0^0	θ_6

In addition, the angle between the axes of joints R_1 and R_7 is 60^0, θ is specified as -45^0 and a_7 is 1.47. Therefore, the pose of end-effector Σ_{EE} with respect to Σ_1 ($\boldsymbol{A}$) can be

obtained (Fig. 3(b)). First, the frame Σ_1 rotates 60^0 about the x-axis ($\boldsymbol{R}_1$), then it moves 1.47 units along the z-axis ($\boldsymbol{P}_2$) and rotates another 60^0 about its x axis ($\boldsymbol{R}_3$), finally we get the frame Σ_{EE} after rotating -45^0 about the z-axis ($\boldsymbol{R}_4$):

$$\boldsymbol{A} = \boldsymbol{R}_1.\boldsymbol{P}_2.\boldsymbol{R}_3.\boldsymbol{R}_4 \quad (5)$$

that is:

$$\boldsymbol{A} = \begin{bmatrix} 1 & 0 & 0 & 0 \\ 0 & 0.7071067810 & 0.7071067810 & 0 \\ -1.273057344 & 0.3535533905 & -0.3535533905 & -0.8660254040 \\ 0.7350000000 & -0.6123724358 & 0.6123724358 & -0.50000000000 \end{bmatrix}$$

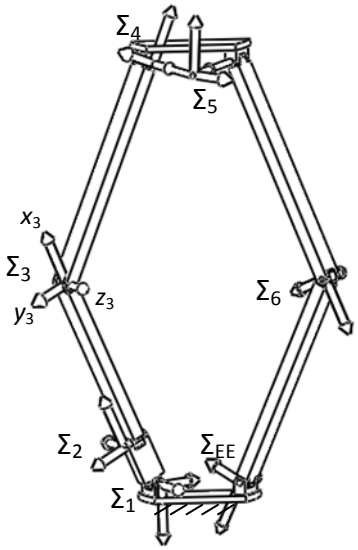

(a) Coordinate frame system for the SLR7RMMOM

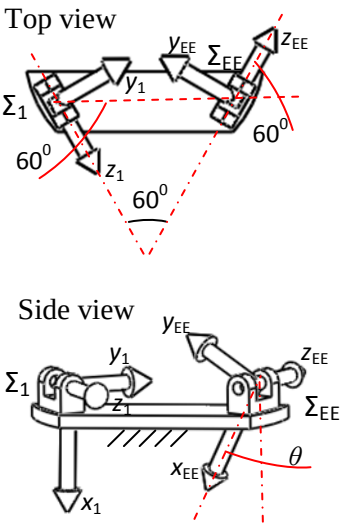

(b) The frame representation for Σ_1 and Σ_{EE}

Fig. 3. Coordinate frame system for the SLR7RMMOM

3.2. Solutions for the kinematic analysis

The algorithm for the inverse kinematics analysis of a general 6R serial manipulator presented in [11-13] mainly used kinematic mapping method. Using this method, an Euclidean displacement can be mapped into a point on a study quadric (S_6^2) in a seven dimensional space, the so called kinematic mapping space P^7, where the point is displayed by eight study parameters. In the kinematic mapping space, the constraint manifold of a 2R-chain is the intersection of a 3-space with the S_6^2, and the constraint manifold of a 3R chain is the intersection of a set of 3-spaces with the S_6^2, where the set of 3-spaces is called Segre Manifold (*SM*).[11] The *SM* of a 3R-chain can be represented by a set of four bilinear equations in the eight homogenous study parameters, which is denoted by z_0, z_1, …, z_7, and one additional parameter corresponding to the tangent half of one joint angle out of the three joint angles. That means that there are three *SMs* (SM_i, i=1, 2, 3) which were presented by three sets of four equations for a 3R-chain.

The 6R serial chain associated with the 1-DOF SLR7RMMOM is further decomposed into two 3R chains, the left 3R one (1-2-3) with end effector frame Σ_L and the right 3R one (6-5-4) with end effector frame Σ_R (Fig. 4). The pose of the frame Σ_L with respect to Σ_1 ($\boldsymbol{T}_L$) and the pose of the frame Σ_R with respect to Σ_1 ($\boldsymbol{T}_R$) can be obtained based on Eqs. (4) and (5):

$$\boldsymbol{T}_L = \boldsymbol{M}_1\boldsymbol{G}_1\boldsymbol{M}_2\boldsymbol{G}_2\boldsymbol{M}_3\,\boldsymbol{G}_3 \quad (6.a)$$

$$\boldsymbol{T}_R = \boldsymbol{A}\boldsymbol{G}_6^{-1}\boldsymbol{M}_6^{-1}\boldsymbol{G}_5^{-1}\boldsymbol{M}_5^{-1}\boldsymbol{G}_4^{-1}\boldsymbol{M}_4^{-1} \quad (6.b)$$

In some discrete, the frames Σ_L and Σ_R have to coincide, which means there is intersection among SM_L, SM_R and S_6^2. The equations for *SMs* the can be derived from Eq. (6). Three sets of four equations can be obtained for the left or the right 3R chain, and each depends on one out of three joint angles.[14] One needs to select one of the three sets of four equations for the left 3R-chain and one of the three sets of four equations for the right 3R-chain according to different situations[14] before doing further calculation.

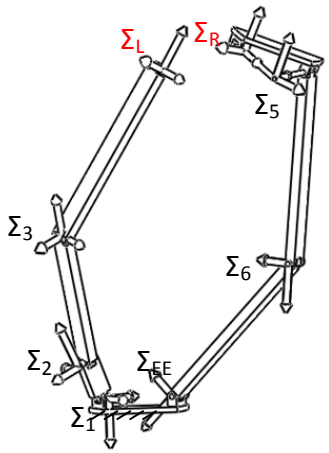

Fig. 4. Decomposing the loop into two 3R chains

In some cases, not all the three *SMs* can be selected [13]. If one select one *SM* depending on one R joint with the joint axes of the remaining two parallel or intersected, which means the *SM* lies on the S_6^2, then the intersection with the S_6^2 fails. Therefore, we select SM_3, which refers to four equations in v_3 (tangent half angle of θ_3), for the left 3R-

chain since the axes of joints R_1 and R_2 do not intersect and are not parallel. For the right 3R-chain, we select SM_5 with four equations in $\bar{v}_5$ (minus tangent half angle of θ_5), because the axes of joints R_4 and R_5 intersect and the axes of joints R_5 and R_6 are parallel. Thus eight equations for the 6R serial mechanism are obtained as follows:

$$h1_{v_3}: 30.4z_0 + 24.0z_1 + 6.4z_2v_3 - 8.0z_4 + 8.0z_5 - 8.0z_6v_3 - 8.0z_7v_3 = 0 \quad (7)$$

$$h2_{v_3}: 30.4z_0 - 24.0z_1 - 6.4z_2v_3 + 8.0z_4 + 8.0z_5 - 8.0z_6v_3 + 8.0z_7v_3 = 0 \quad (8)$$

$$h3_{v_3}: 6.4z_1v_3 - 24.0z_2 - 30.4z_3 - 8.0z_4v_3 + 8.0z_5v_3 + 8.0z_6 + 8.0z_7 = 0 \quad (9)$$

$$h4_{v_3}: -6.4z_1v_3 + 24.0z_2 + 30.4z_3 + 8.0z_4v_3 + 8.0z_5v_3 + 8.0z_6 - 8.0z_7 = 0 \quad (10)$$

$$h5_{\bar{v}_5}: z_0(2.72626795828513 - 6.58179306856969\bar{v}_5) + z_1(4.12012622455083 - 4.85463523903963\bar{v}_5) + z_2(8.65463523574647 - 5.69413776088330\bar{v}_5) + z_3(-1.37687417023358^{-9} + 4.47457271235407^{-9}\bar{v}_5) + z_4(-1.24264068742686 - 3.00000000128678\bar{v}_5) + z_5(0.717438935080522 + 1.73205080649897\bar{v}_5) + z_6(1.73205080649897 - 0.717438935080522\bar{v}_5) + z_7(3.00000000128678 - 1.24264068742628\bar{v}_5) = 0 \quad (11)$$

$$h6_{\bar{v}_5}: z_0(-2.7262679415240 + 6.58179306736930\bar{v}_5) + z_1(0.972103152392334 + 2.74536476831045\bar{v}_5) + z_2(8.65463523588648 + 5.69413776432743\bar{v}_5) + z_3(3.07322256531961^{-9} + 1.01209529645985^{-9}\bar{v}_5) + z_4(-0.414213562192757 - 0.99999999133379\bar{v}_5) + z_5(-0.717438935213303 - 1.73205080788068\bar{v}_5) + z_6(1.73205080788068 - 0.717438935213303\bar{v}_5) + z_7(-0.99999999133379 + 0.414213562192757\bar{v}_5) = 0 \quad (12)$$

$$h7_{\bar{v}_5}: z_0(1.37687550250121^{-9} - 4.47457315644328^{-9}\bar{v}_5) + z_1(-8.65463523574647 - 5.69413776088330\bar{v}_5) + z_2(-4.12012622455083 + 4.85463523903963\bar{v}_5) + z_3(2.72626795828513 - 6.58179306856969\bar{v}_5) + z_4(-3.00000000128678 + 1.24264068742628\bar{v}_5) + z_5(1.73205080649897 - 0.717438935080522\bar{v}_5) + z_6(-0.717438935080522 - 1.73205080649897\bar{v}_5) + z_7(-1.24264068742686 - 3.00000000128678\bar{v}_5) = 0 \quad (13)$$

$$h8_{\bar{v}_5}: z_0(-3.07322167714119^{-9} - 1.01209551850445^{-9}\bar{v}_5) + z_1(8.65463523588648 + 5.69413776432743\bar{v}_5) + z_2(-0.972103152392334 - 2.74536476831045\bar{v}_5) + z_3(-2.7262679415240 + 6.58179306736930\bar{v}_5) + z_4(0.99999999133379 - 0.414213562192757\bar{v}_5) + z_5(1.73205080788068 - 0.717438935213303\bar{v}_5) + z_6(0.717438935213303 + 1.73205080788068\bar{v}_5) + z_7(-0.414213562192757 - 0.99999999133379\bar{v}_5) = 0 \quad (14)$$

$$h9: z_0z_4 + z_1z_5 + z_2z_6 + z_3z_7 = 0 \quad (15)$$

Including the equation for the S_6^2 shown in Eq. (15), we obtain nine bilinear equations in ten unknowns (Eqs. (7)-(15)). Because z_0, z_1, …, z_7 are homogeneous, so one of them can be normalize to 1. Solving seven of the nine equations to get the eight study parameters for z_0, z_1, …, z_7 in v_3 and $\bar{v}_5$, and substituting the solutions into the remaining two equations, we obtain two equations in v_3 and $\bar{v}_5$ named E_1 and E_2 as

$$E_1: v_3^4\bar{v}_5^4 + 3.640783761v_3^4\bar{v}_5^3 - 3.788653411v_3^3\bar{v}_5^4 - 7.000053530v_3^4\bar{v}_5^2 + 10.71593007v_3^3\bar{v}_5^3 + 41.87086614v_3^2\bar{v}_5^4 + 3.640783761v_3^4\bar{v}_5 - 19.64341956v_3^2\bar{v}_5^3 - 3.788653411v_3\bar{v}_5^4 - 0.5952224873v_3^4 - 10.71593007v_3^3\bar{v}_5 - 79.84271214v_3^2\bar{v}_5^2 + 10.71593007v_3\bar{v}_5^3 + 11.40205846\bar{v}_5^4 + 3.788653411v_3^3 - 19.64341956v_3^2\bar{v}_5 - 23.28420332\bar{v}_5^3 + 53.83503480v_3^2 - 10.71593007v_3\bar{v}_5 - 131.7802740\bar{v}_5^2 + 3.788653411v_3 - 23.28420332\bar{v}_5 + 24.96144960 = 0 \quad (16)$$

$$E_2: v_3^8\bar{v}_5^6 - 3.975059020v_3^8\bar{v}_5^5 - 9.917459999v_3^7\bar{v}_5^6 + 4.782767392v_3^8\bar{v}_5^4 + 10.89653630v_3^7 - 7.905713714v_3^6\bar{v}_5^6 - 2.187051780v_3^8\bar{v}_5^3 + 10.76914366v_3^7\bar{v}_5^4 + 11.58607438v_3^6\bar{v}_5^5 - 1.756500002v_3^5\bar{v}_5^6 + 0.1775892990v_3^8\bar{v}_5^2 - 6.718456391v_3^8 - 19.63855979v_3^6\bar{v}_5^4 - 3.599595703v_3^5\bar{v}_5^5 + 5.541460022v_3^4\bar{v}_5^6 + 0.1309074494v_3^8\bar{v}_5 - 10.68103759v_3^7\bar{v}_5^2 + 29.42980884v_3^6\bar{v}_5^3 + 88.38390043v_3^5\bar{v}_5^4 + 14.52156887v_3^4\bar{v}_5^5 - 11.11952017v_3^3\bar{v}_5^6 - 0.02663720154v_3^8 + 8.366957525v_3^7\bar{v}_5 + 1.744100557v_3^6\bar{v}_5^2 - 11.42375341v_3^5\bar{v}_5^3 + 47.03555747v_3^4\bar{v}_5^4 + 27.82871185v_3^3\bar{v}_5^5 + 23.16294757v_3^2\bar{v}_5^6 - 1.555454321v_3^7 - 14.97543807v_3^6\bar{v}_5 - 65.86121591v_3^5\bar{v}_5^2 + 22.54006617v_3^4\bar{v}_5^3 + 85.76873039v_3^3\bar{v}_5^4 - 19.01000389v_3^2\bar{v}_5^5 - 19.28048017v_3\bar{v}_5^6 + 4.289038591v_3^6 - 39.78294461v_3^5\bar{v}_5 - 55.12245682v_3^4\bar{v}_5^2 - 45.28245200v_3^3\bar{v}_5^3 + 12.06466530v_3^2\bar{v}_5^4 + 42.32484385v_3\bar{v}_5^5 + 8.715773829\bar{v}_5^6 - 4.399164900v_3^5 - 61.91885268v_3^4\bar{v}_5 - 206.5453764v_3^3\bar{v}_5^2 - 104.7180132v_3^2\bar{v}_5^3 + 8.153973623v_3\bar{v}_5^4 - 17.97043737\bar{v}_5^5 + 7.841437590v_3^4 - 127.7979408v_3^3v_3 - 166.3482520v_3^2\bar{v}_5^2 - 40.57715498v_3\bar{v}_5^3 - 59.39221935\bar{v}_5^4 - 2.488637296v_3^3 - 46.57694731v_3^2\bar{v}_5 - 151.3651980v_3\bar{v}_5^2 - 95.64121876\bar{v}_5^3 + 8.367254171v_3^3 - 79.64803864v_3\bar{v}_5 - 109.6592839\bar{v}_5^2 + 0.3550732836v_3 + 0.2355598536\bar{v}_5 + 4.481492373 = 0 \quad (17)$$

Using the resultant to eliminate $\bar{v}_5$ from Eqs. (16) and (17), one polynomial equation of degree 56 in v_3 named E can be derived as follows.

$$E: (v_3{}^2+1)^6(3.033362327v_3{}^4-12.05533640v_3{}^2+10.67784416)(1.87522003v_3{}^4-64.00268390v_3{}^2-387.9596900)(5.157957061\times10^9v_3{}^{10}+1.823061353\times10^{20}v_3{}^9-7.297142808\times10^{21}v_3{}^8+1.634647033\times10^{22}v_3{}^7+5.885504960\times10^{22}v_3{}^6-3.150969451\times10^{22}v_3{}^5-2.671416502\times10^{23}v_3{}^4-2.874236074\times10^{22}v_3{}^3+1.076318546\times10^{23}v_3{}^2+1.893149796\times10^{22}v_3+1.422425962\times10^{23})^2(6.60154501\times10^8v_3{}^{16}+2.698070325\times10^{18}v_3{}^{15}-3.778024642\times10^{28}v_3{}^{14}-8.52528086\times10^{37}v_3{}^{13}+6.145569255\times10^{47}v_3{}^{12}-4.007107158\times10^{49}v_3{}^{11}+2.109260812\times10^{50}v_3{}^{10}+3.306274920\times10^{49}v_3{}^9+5.471487282\times10^{50}v_3{}^8+1.795904346\times10^{51}v_3{}^7-1.709576046\times10^{50}v_3{}^6-2.604353812\times10^{50}v_3{}^5-8.358864852\times10^{50}v_3{}^4-1.755833276\times10^{51}v_3{}^3+2.679828670\times10^{50}v_3{}^2+2.273726304\times10^5v_3-1.982814399\times10^{49})=0 \quad (18)$$

The solutions to $(v_3{}^2+1)^6=0$ are $v_3=\pm I$ (I is the unit imaginary number). The corresponding points in P^7 lie on the exceptional generator, which have to be cut out of the $S_6{}^2$. The solutions of polynomial of 10 degrees squared are points with coordinate (0, 0, 0, 0, 0, 0, 0, 0), which do not lie on the $S_6{}^2$ and the solutions of polynomials of degree 4 are points lie on the exceptional 3-space of the $S_6{}^2$.[13] Then the polynomial of degree 16 gives the 16 solutions:

v_3=[0.08366283786, 0.3610109062, 1.000000000, 6.521970015, 59.40599134, 4.132441204× 10^9, 5.081725257× 10^9, 0.4234204659+2.169839731 I, −0.07511185210+1.019253419 I, −6.650597562× 10^9+3.156689159× 10^8 I, −0.3581658035, −1.000000001, −1.507896627, −6.650597562× 10^9 −3.156689159× 10^8 I, −0.07511185210−1.019253419 I, 0.4234204659−2.169839731 I]

Then the solutions for v_3 are substituted back to E_1 and E_2, the common solutions for $\bar{v}_5$ with their corresponding v_3 are the solutions as desired. Please note only 12 sets of solutions could be easily obtained where the remaining four solutions for v_3 tend to be infinite, such as 5.081725257× 10^9, i.e. θ_3 approaches to be 180^0. The situation that $\theta_3=180^0$ does exist when the joints on the platform and the base coincide. It is special configurations for the 1-DOF SLR7RMMOM, as shown in Fig. 5(i).

The remaining four joint angles for the normal 12 sets of solutions could be solved by the other sets of four equations for SM_1, SM_2, SM_4 and SM_6.

As to the above four particularly configurations in which v_3 tend to be infinite, there is one set of real solutions: $\theta_2=0^0$, $\theta_3=180^0$, $\theta_6=180^0$, θ_1, θ_4 and θ_5 can be any value. This set of solutions can be easily verified by observation. The complex solutions associated with the remaining three particularly configurations are omitted in this paper.

Finally, 13 sets of solutions for the forward kinematics analysis of the single loop are obtained, as listed in Table 2.

Table 2. Solutions for the loop

Solutions	θ_1(deg)	θ_2(deg)	θ_3(deg)	θ_4(deg)	θ_5(deg)	θ_6(deg)
Solution 1	−173.940	20.726	9.565	−3.504	−155.426	−45.598
Solution 2	135.000	0.000	90.000	−45.000	−135.000	−90.000
Solution 3	−135.000	0.000	−90.000	45.000	−135.000	−90.000
Solution 4	−4.576	15.737	178.071	−2.648	−70.339	−172.852
Solution 5	−78.354	118.963	−112.897	−145.457	86.692	−119.924
Solution 6	−154.651	73.117	39.700	−14.351	131.208	90.703
Solution 7	−25.162	72.737	−39.412	−165.750	−41.899	90.473
Solution 8	141.385	−94.455	162.566	158.819	156.631	−137.538
Solution 9	−54.493−109.370I	163.879+10.798I	−106.507−186.806I	−127.985+77.436I	58.785+82.626I	−100.688−144.387I
Solution 10	−54.493+109.370I	163.879−10.798I	−106.507+186.806I	−127.985−77.436I	58.785−82.626I	−100.688+144.387I
Solution 11	93.401+63.964I	−142.300+1.679I	167.711+54.093I	105.690+9.871I	112.781+77.655I	−156.361−28.617I
Solution 12	93.401−63.964I	−142.300−1.679I	167.711−54.093I	105.690−9.871I	112.781−77.655I	−156.361+28.617I
Solution 13	Any value	0.000	180.000	Any value	Any value	180.000

Note: I is the unit imaginary number

The above real solutions for the kinematic analysis have been verified using the CAD models for the 1-DOF SLR7RMMOM. The CAD configurations associated with these solutions are shown in Fig. 5.

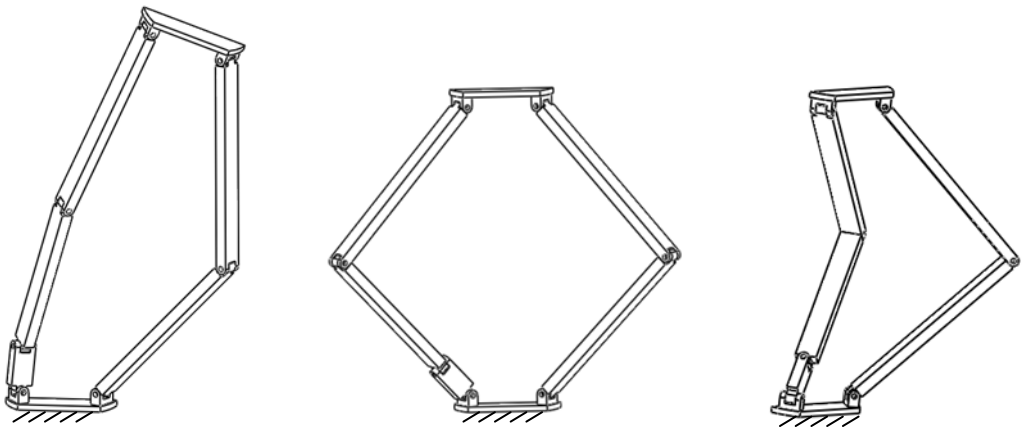

(a) Solution 1: θ_3=9.565^0 (b) Solution 2: θ_3=90.000^0 (c) Solution 3: θ_3=−90.000^0

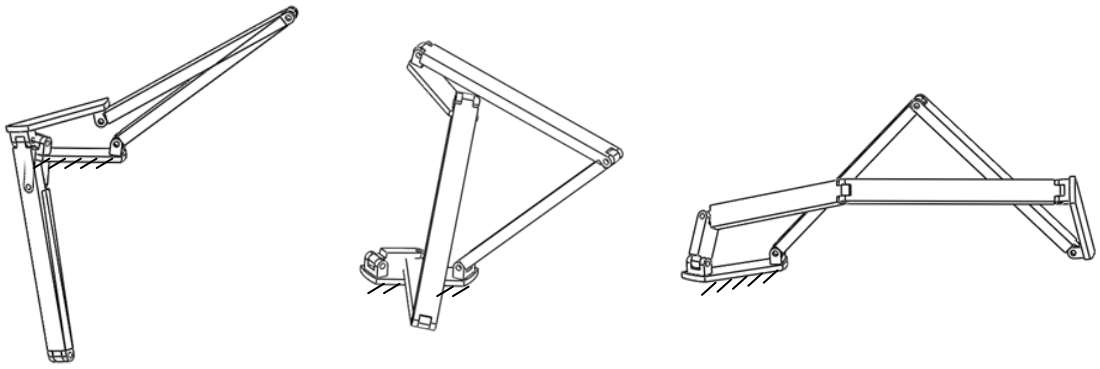

(d) Solution 4: θ_3=178.071^0 (e) Solution 5: θ_3=−112.897^0 (f) Solution 6: θ_3=39.700^0

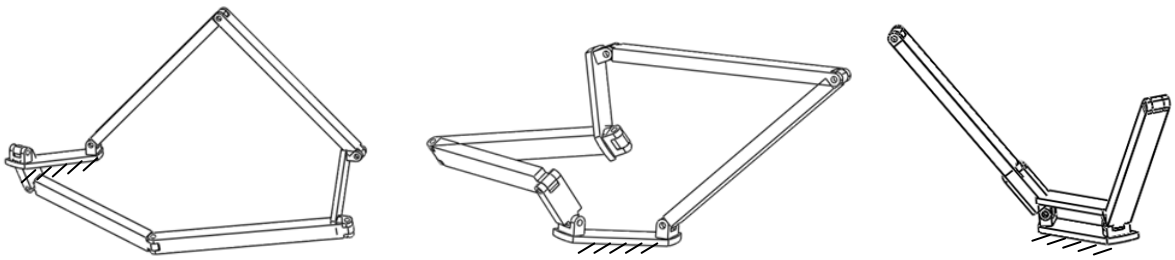

(g) Solution 7: θ_3=−39.412^0 (h) Solution 8: θ_3=162.566^0 (i) Solution 13: θ_3=180.000^0

Fig. 5. CAD configurations corresponding to the real solutions

4. Operation Modes and Transitional Configurations

As the input angle θ changes, a series of solutions corresponding to different input angles can be obtained accordingly. Then via plotting the joint angles against the input angle, we illustrate the operation modes and transitional configurations of the 1-DOF SLR7RMMOM (Fig. 6). All the operation modes and transitional configurations of the mechanism can be obtained from the plotting of angles θ_1 and θ_3 against the input angle θ.

Figure 6 shows that there are two straight lines A and B and two closed curves C (C_0-C_1-C_2-C_0 in Fig. 6(a) or C_0-C_1-C_2-C_3-C_4-C_0 in Fig. 6(b)) and D (D_0-D_1-D_2-D_3-D_4-D_0) designating the operations modes. Lines A and B are associated with translation operation mode, while the closed curves C and D are associated with two 1-DOF planar operation modes separately. Therefore, the mechanism has three operation modes but not only two operation modes. This could be easily verified by comparing the straight lines and closed curves to their corresponding operation mode figures in Fig. 5. Line A corresponds to Fig. 5(b), Line B corresponds to Fig. 5(c), closed curve C corresponds to Fig. 5(a), and closed curve D corresponds to Fig. 5(f).

In the following, the transitional configurations between three operation modes are analyzed. By comparing the two plotting figures (Fig. 6), two intersecting points TA and TB, through which both operation modes pass in both the plotting figures are apparently observed, which represent the transitional configurations (Fig.7). The input angles corresponding to the transitional configurations are shown in Table 3.

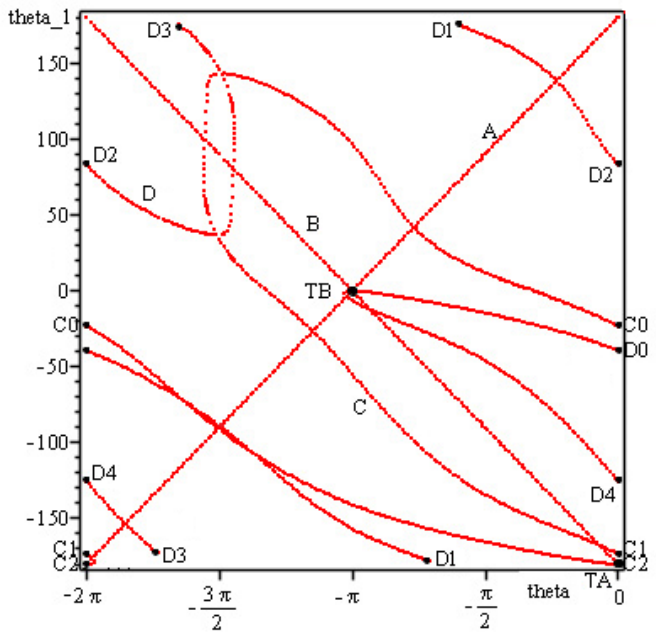

(a)

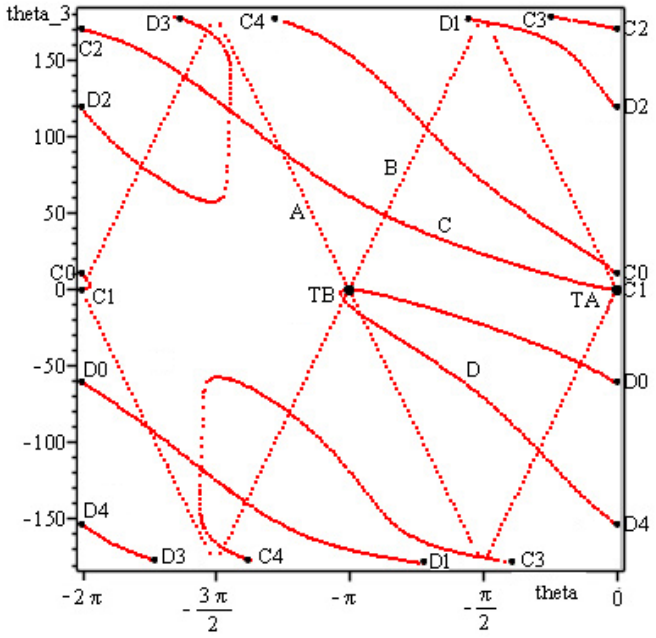

(b)

Fig. 6. Plotting of two rotational angles (θ_1 and θ_3) against input angle θ: a) θ_1 (deg) in vertical axis versus θ (rad) in the horizontal axis; b) θ_3 (deg) in vertical axis versus θ (rad) in the horizontal axis

Table 3. Transitional configurations

Transition points	Input angle θ in degree	Modes
TA	0^0	Translational mode & 1-DOF planar mode one (curve C)
TB	180^0	Translational mode & 1-DOF planar mode two (curve D)

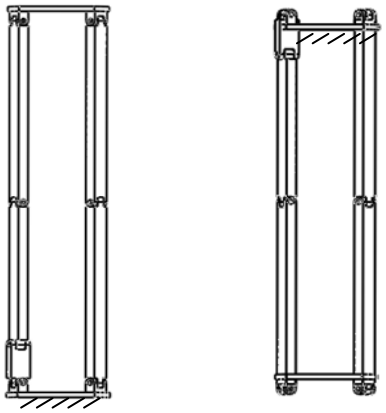

(a) TA: $\theta=0^0$ (b) TB: $\theta=180^0$

Fig. 7. Transitional configurations of the SLR7RMMOM.

5. Conclusions

The kinematics analysis of a novel 1-DOF SLR7RMMOM has been implemented. Using the algorithm for the inverse kinematics of a general serial 6R manipulator, a set of solutions for the 1-DOF SLR7RMMOM have been obtained with the real solutions verified through the CAD model of the mechanism. The solutions against a series of input angle have been plotted in two figures, which show that the mechanism has three operation modes: translational mode and two 1-DOF planar modes. Transitional configurations have also been identified where the mechanism can switch from one operation mode to another.

When switching the proposed 1-DOF SLR7RMMOM from one operation mode to another, neither the extra actuator nor disassembly is needed. Therefore, this reconfigurable mechanism may be useful for developing energy-efficient manipulators.

The investigation of the operation modes of the mechanism using an algebraic approach[15] instead of the numerical approach deserves further application.

Acknowledgement

The authors would like to thank the Royal Society, United Kingdom for the financial support through an International Joint Project No. JP100715. X. He would like to acknowledge the financial support from the SORSAS PhD scholarship in Heriot-Watt University. Special thanks go to Prof. M.L. Husty and Dr. M. Pfurner in Universität Innsbruck, Austria for their valuable help in using their kinematic mapping algorithms.

References

1. Yang, G., Chen, I., Lim, K.M., Huat, Y.S., 1999, "Design and Kinematic Analysis of Modular Reconfigurable Parallel Robots", *1999 IEEE Conference on Robotics and Automation*, May, 1999, Detroit, MI, US.
2. Yang, G., Chen, W., Chen, Y., Huat, Y.S., Chen, G., 2001, *"Design and Kinematic Analysis of Modular Reconfigurable Parallel Robot"*, Springer, Vol.**10**: 83-89.

3. Kuo, C., Dai, J., 2009, "Reconfiguration Principles and Strategies for Reconfigurable Mechanisms", *ASME/IFToMM International Conference on Reconfigurable Mechanisms and Robots,* June 2009, London, UK.
4. Galletti, C., Fanghella, P., 2001, "Single-loop Kinematotropic Mechanism", *Mechanism and Machine Theory*, Vol. **36**: 743-761.
5. Rakotomanga, N., Chablat, D.,Caro, S., "Kinatostatic Performance of a Planar Mechanism with Variable Actuation", *Jadran Lenarcic and philippe Wenger, Advances in Robot Kinematics: Analysis and Design*, pp. 311-320.
6. Kong, X., Huang, C., 2009, "Type Synthesis of Single-DOF Single-loop Mechanisms with Two Operation Modes", *ASME/IFToMM International Conference on Reconfigurable Mechanisms and Robots*, June 2009, London, UK.
7. Kong, X., Type synthesis of 3-DOF parallel manipulators with both planar and translational operation modes. Proceedings of ASME 2011 International Design Engineering Technical Conferences & Computers and Information in Engineering Conference, DETC2011-48510, Washington, USA, August 28-31, 2011.
8. Zlatanov, D., Bonev, I.A., Gosselin, C.M., 2002, "Constraint Singularity as C-Space Singularities", *Advances in Robot Kinematics-Theory and Application*, J. Lenarčič and F. Thomas eds., Kluwer Academic Publishers, pp. 183-192.
9. Wang, X., Hao, M., Cheng, Y., 2008, "On the Use of Different Evaluation for Forward Kinematics of Parallel Manipulators", *Applied Mathematics and Computation*, Vol. **25**: 760-769.
10. Bonev, I.A., Zlatanov, D., Gosselin, C.M., 2003, "Singularity Analysis of 3-DOF Planar Parallel Mechanisms via Screw Theory", *Journal of Mechanical Design*, Vol. **125**.
11. Husty, M.L., Pfurner, M., Schrocker, H.P., 2007, "A New and Effective Algorithm for the Inverse Kinematics of a General Serial 6R Manipulator", *Mechanism and Machine Theory*, Vol. **42**: 66-81.
12. Husty, M.L., Pfurner, M., Schrocker, H.P., Brunnthaler, K., 2007, "Algebraic Method in Mechanism Analysis and Synthesis", *Robotica*, Cambridge University Press, Vol. **25**: 661-675.
13. Pfurner, M., 2006, "*Analysis of Spatial Serial Manipulators Using Kinematic Mapping*", PhD Thesis, University of Innsbruck, Austria.
14. Kong, X., and Gosselin, C.M., Type Synthesis of Parallel Mechanisms. Springer, 2007.
15. Pfurner, M., 2012, Multiple-Mode Closed 7-Link Chains Based on Overconstrained 4-Link Mechanisms, New Trendes in Mechanism and Machine Science, Springer, pp. 73-81.